ELSEVIER

Biochimica et Biophysica Acta 1281 (1996) 80–90

BBA Biochimica et Biophysica Acta

Functional expression of the cystic fibrosis transmembrane conductance regulator in yeast

Pingbo Huang [a], Katarina Stroffekova [b,d], John Cuppoletti [b,c], Sanjoy K. Mahanty [a], Gene A. Scarborough [a,*]

[a] *Department of Pharmacology, Campus Box #7365, FLOB, University of North Carolina at Chapel Hill, Chapel Hill, NC 27599, USA*
[b] *Department of Molecular and Cellular Physiology, University of Cincinnati, Cincinnati, OH 45267, USA*
[c] *Department of Internal Medicine, University of Cincinnati, Cincinnati, OH 45267, USA*
[d] *Institute of Molecular Physiology and Genetics Slovak Academy of Sciences, Bratislava, Slovak Republic*

Received 29 September 1995; accepted 23 January 1996

Abstract

Recombinant human cystic fibrosis transmembrane conductance regulator (CFTR) has been produced in a *Saccharomyces cerevisiae* expression system used previously to produce transport ATPases with high yields. The arrangement of the bases in the region immediately upstream from the ATG start codon of the CFTR is extremely important for high expression levels. The maximal CFTR expression level is about 5–10% of that in Sf9 insect cells as judged by comparison of immunoblots. Upon sucrose gradient centrifugation, the majority of the CFTR is found in a light vesicle fraction separated from the yeast plasma membrane in a heavier fraction. It thus appears that most of expressed CFTR is not directed to the plasma membrane in this system. CFTR expressed in yeast has the same mobility (ca. 140 kDa) as recombinant CFTR produced in Sf9 cells in a high resolution SDS-PAGE gel before and after *N*-glycosidase F treatment, suggesting that it is not glycosylated. The channel function of the expressed CFTR was measured by an isotope flux assay in isolated yeast membrane vesicles and single channel recording following reconstitution into planar lipid bilayers. In the isotope flux assay, protein kinase A (PKA) increased the rate of $^{125}I^-$ uptake by about 30% in membrane vesicles containing the CFTR, but not in control membranes. The single channel recordings showed that a PKA-activated small conductance anion channel (8 pS) with a linear *I–V* relationship was present in the CFTR membranes, but not in control membranes. These results show that the human CFTR has been expressed in functional form in yeast. With the reasonably high yield and the ability to grow massive quantities of yeast at low cost, this CFTR expression system may provide a valuable new source of starting material for purification of large quantities of the CFTR for biochemical studies.

Keywords: Cystic fibrosis transmembrane conductance regulator; Yeast; Expression; Initiation codons; Chloride ion channel

1. Introduction

The cystic fibrosis transmembrane conductance regulator (CFTR) is the protein product of the gene associated with cystic fibrosis, a lethal genetic disease. Extensive biochemical and biophysical studies have been carried out with the CFTR as a therapy target and a novel channel. A variety of biochemical approaches to obtaining a more detailed understanding of the structure and function of the CFTR will require large quantities of purified functional protein. Since the endogenous levels of CFTR in human tissues are low, suitable starting material for CFTR purification is only available from high-yield heterologous expression systems. Thus far, the Sf9 insect cell/baculovirus expression system has provided the largest amount of starting material for CFTR purification, and functional CFTR has been purified using this system [1,2]. However, the insect cell system and other available heterologous systems employing animal cells involve relatively complicated culture techniques and expensive media. In contrast, yeast expression systems have the potential to generate massive quantities of eukaryotic proteins at low cost be-

Abbreviations: CFTR, cystic fibrosis transmembrane conductance regulator; EDTA, ethylenediamine-tetraacetic acid; HEPES, *N*-(2-hydroxyethyl)piperazine-*N'*-(2-ethanesulfonic acid); PVDF, polyvinylidene difluoride; PKA, cAMP-dependent protein kinase; SDS-PAGE, sodium dodecyl sulfate-polyacrylamide gel electrophoresis; Sf9 cells, *Spodoptera frugiperda* cultured ovarial cells.

* Corresponding author. Fax: +1 (919) 9665640.

PII S0005-2736(96)00032-6

cause of their simple culture requirements. Another advantage of yeast expression systems is that thoroughly developed and readily manipulated yeast genetics can provide novel experimental approaches for studying the expressed proteins, which is much more difficult in animal and insect cell expression systems. We have recently reported high-yield expression of the neurospora plasma membrane H^+-ATPase [3] using the yeast expression system developed by Serrano and his co-workers [4]. This system utilizes the strong promoter of the yeast plasma membrane H^+-ATPase, and has been used to express several eukaryotic H^+-ATPases in high yields [3,4]. The success of these studies prompted us to attempt to obtain expression of the CFTR in this system. Relatively low levels of CFTR expression were immediately detected, and additional changes in the bases preceding the ATG start codon of the CFTR led to a marked increase in expression levels. In this article, these studies are described and the properties of the CFTR produced are characterized. This new CFTR expression system should provide a valuable source of starting material for purification of large amounts of the CFTR. Moreover, the results obtained suggest that this system may be useful in the development of high-yield expression systems for other membrane proteins.

2. Materials and methods

2.1. Plasmid construction and site-directed mutagenesis

Construction of pHCFTR + started with the yeast expression vector pSKMHA1 [3], and the baculovirus transfer vector pVL-atgCFTR, which contains the full-length human CFTR cDNA. pVL-atgCFTR was derived from the baculovirus vector described previously by Sarkadi et al. [5], by removing the region (36 base pairs) between the ATG start codon of the CFTR and the upstream *Not*I site in an attempt to improve insect cell expression levels (Nemecz, S. and Scarborough, G.A., unpublished results). In order to introduce the CFTR cDNA of pVL-atgCFTR into pSKMHA1, a new *Not*I-*Xba*I fragment was generated using the polymerase chain reaction with pVL-atgCFTR as template and appropriate primers. This new fragment contained the 16 base pairs upstream of the ATG start codon of the H^+-ATPase cDNA in pSKMHA1, including a *Not*I site [3], followed by a 513 base pair fragment of the CFTR cDNA beginning at the ATG start codon and extending to an *Xba*I site that had previously been silently inserted in the coding region of the CFTR [5]. Another fragment from the *Xba*I site in the CFTR coding region to a *Not*I site downstream from the CFTR stop codon in pVL-agtCFTR, was ligated with this new fragment and the non-ATPase *Not*I-*Not*I fragment of pSKMHA1. This three-way ligation generated two types of plasmids because of the *Not*I site at both ends of the CFTR insert. The construct with the CFTR cDNA present in the sense direction was designated pHCFTR + . The construct with the CFTR cDNA present in the antisense direction was designated pHCFTR − . Standard recombinant DNA techniques [6] were used for the plasmid constructions.

Following the construction of pHCFTR + , site-directed mutagenesis was carried out on this plasmid to construct plasmids pHCFTR1, pHCFTR2, pHCFTR3, pHCFTRS and pHCFTRW. For pHCFTR1, pHCFTR2, pHCFTR3 and pHCFTRS, the *Sac*I to *Not*I cassette in pHCFTR + was used for mutagenesis. Because of the lack of a *Not*I site in the M13mp19 vector, this cassette was first subcloned into pBluescript in order to introduce an *Xba*I site that is compatible with the M13mp19 vector. Then the *Sac*I to *Xba*I fragment containing the *Sac*I to *Not*I cassette in pBluescript was subcloned into the M13mp19 vector. Mutagenesis was then carried out as described by Kunkel [7]. The mutated *Sac*I to *Not*I cassettes in the M13mp19 were then ligated into pHCFTR + to replace its corresponding wild type cassette. For pHCFTRW, the *Sac*I to *Nru*I cassette was used for mutagenesis. Because *Nru*I is a blunt-end restriction enzyme and is destroyed after subcloning into M13mp19, the *Sac*I to *Xho*I fragment containing the cassette was used for subcloning into M13mp19. The mutated *Sac*I to *Nru*I fragment in M13mp19 was then ligated into pHCFTR + to replace its corresponding wild-type cassette. All mutated cassettes were sequenced completely to confirm that only the designed mutation had occurred, and all mutations were verified by again sequencing the appropriate regions in the final plasmids before yeast transformation.

2.2. Yeast transformation

Transformation of the yeast cells was carried out as described previously [3]. Transformation of yeast strain EGY48 with plasmids pHCFTR + , pHCFTR − , pHCFTR1, pHCFTR2, pHCFTR3, pHCFTRS, and pHCFTRW gave rise to yeast strains HCFTR + , HCFTR − , HCFTR1, HCFTR2, HCFTR3, HCFTRS, and HCFTRW, respectively.

2.3. Yeast strain and growth media

S. cerevisiae strain EGY48 (*MATα, his3, trp1, ura3-52, leu2::pLEU2-LexAop6*) was grown on synthetic medium containing 2% (w/v) glucose and 0.7% (w/v) yeast nitrogen base without amino acids, supplemented with 0.4 mM L-histidine, 0.4 mM uracil, 0.4 mM L-tryptophan, and 1 mM L-leucine. Leucine was omitted for the selection and growth of transformants. Solid media additionally contained 2% (w/v) Difco agar. For the preparation of membrane vesicles, the transformants were grown at 30°C in the synthetic medium to stationary phase (about 40–48 h), diluted 20-fold in the same medium, and grown for an additional 24 h. Cells were harvested by centrifugation and used for preparation of membrane vesicles.

2.4. Isolation of membrane vesicles

The yeast membrane vesicle isolation procedure was essentially the same as described [3], with minor modifications. The homogenization buffer contained 28 mM Tris, 0.2 M sucrose, 5.4 mM EDTA, 1 mM phenylmethylsulfonyl fluoride, 2 μg/ml chymostatin, and 5 μg/ml leupeptin, pepstatin and aprotinin, pH 8.5 with HCl. A 10% (w/v) NaCl solution/ice slurry (freezing point about −10°C) was used as a coolant for the glass beads homogenizer. The membrane pellet collected after 146000 × *g* centrifugation was resuspended in a storage buffer the same as the homogenization buffer except that its pH was 7.4. The membrane vesicle suspension was aliquoted and stored at −80°C. The protein concentration was 10–12 mg/ml.

2.5. SDS-PAGE and immunoblotting

SDS-PAGE electrophoresis and immunoblotting were carried out essentially as described by Sarkadi et al. [5]. Electrophoresis was usually carried out in 7.5% SDS-PAGE mini gels in a Bio-Rad Mini-Protean II electrophoresis cell. In some cases, the electrophoresis was carried out in 15 × 15 × 0.075-cm gels in a Hoefer electrophoresis cell for high resolution. For immunostaining of the CFTR, the first and second antibodies were 1:500 diluted monoclonal mouse anti-human CFTR (R domain specific, Genzyme) and anti-mouse Ig, peroxidase-linked whole antibody from sheep (Amersham), respectively. For the yeast plasma membrane ATPase, 1:100000 diluted polyclonal antiserum [8] to the yeast ATPase was used with anti-rabbit Ig, peroxidase-liked whole antibody from donkey as the second antibody (Amersham).

2.6. Subcellular distribution of the expressed CFTR

Membrane vesicles were prepared as described above, except that the 0.2 M sucrose was omitted from the storage buffer. The crude membrane suspension was diluted to 1.5 mg protein/ml with the non-sucrose storage buffer, and 2-ml aliquots were layered on top of a discontinuous sucrose gradient containing 2 ml aliquots of 45%, 40%, 35%, 30% and 25% (w/v) sucrose in the same buffer in a 12-ml centrifuge tube. The gradients were centrifuged at 150000 × *g* at 4°C for 3 h in a Beckman SW 40 Ti rotor, and the supernatant fluids and the membrane layers on the top of each layer were collected (0.6 ml fractions) and assayed for protein concentration. Twenty μg of protein from each fraction was precipitated with 4% (w/v) trichloroacetic acid in the presence of 0.2 mg/ml bovine serum albumin, and the precipitates were dissolved in 20 μl of disaggregation buffer and subjected to SDS-PAGE and immunoblotting for the CFTR. After a luminogram of immunostaining for the CFTR had been obtained, the same blot was washed for 1 h in TBS-Tween buffer [5] and reblotted for the yeast plasma membrane H^+-ATPase.

2.7. $^{125}I^-$ uptake assay

Chloride channel activities were determined by the $^{125}I^-$ uptake assay described by Ran and Benos [9]. Frozen vesicle suspensions (45 μl, 10 mg protein/ml) were thawed and mixed with 335 μl of a hypotonic solution to produce a hypotonic shock to increase the chances that protein kinase A (PKA) gained access to both sides of the membrane vesicles. The hypotonic solution contained 20 mM Tris, 1 mM $MgCl_2$, 10 mM NaF (phosphatase inhibitor), 10 mM MgATP, 1 mM ATP-γ-S, 200 μM Na_3VO_4, 5 μg/ml chymostatin, leupeptin, pepstatin, and aprotinin, pH 7.2 with HCl, and 2 μl PKA solution (catalytic subunit, Promega, final concentration 280 nM). In control experiments, 2 μl of the PKA solution was replaced by 2 μl of PKA control solution (Promega's buffer for PKA catalytic subunit, 350 mM K phosphate and 0.1 mM DL-dithiothreitol, pH 6.8). ATP-γ-S was used because it serves as a substrate for PKA in the phosphorylation reaction, but the transferred thiophosphate is not readily removed by protein phosphatases [10]. Na_3VO_4 was used as an inhibitor of phosphatases and P-type ATPases. After 10 min incubation at 30°C, the mixture was mixed with 20 μl of 3 M KCl to produce a final KCl concentration of 150 mM. The mixture was incubated for 40 min on ice and again for 10 min at 30°C. In order to remove external Cl^- and generate an inside-positive diffusion potential for driving external $^{125}I^-$ into the vesicles, the mixture was passed though a 2-ml Sephadex G-50 column and eluted with 800 μl of ice-cold elution buffer (0.3 M sucrose, 10 mM Hepes, 1 mM $MgCl_2$, pH 7.2 with Tris). The Sephadex column was equilibrated with ice-cold elution buffer before use. The 800 μl eluate from the Sephadex G-50 column was then mixed with 10 μl 20 mM Na_3VO_4, 10 μl 200 mM ATP, and 4 μl PKA catalytic subunit (final 280 nM) or PKA control solution. $^{125}I^-$ uptake was initiated by adding 10 μCi of $Na^{125}I$ (carrier-free, Amersham) on ice. At time 0, 3 and 6 min, 120 μl aliquots were removed from the mixture and passed though 2 ml Dowex 1X8-100 columns (Cl^- form) and eluted with 1 ml of the elution buffer described above (ice-cold). The Dowex 1X8-100 columns were washed with 2 ml ice-cold elution buffer and stored at 0°C before use. The $^{125}I^-$ radioactivity in the eluate was counted directly in a gamma counter with less than 2% counting error.

2.8. Single channel recordings

The single channel recording procedure was essentially the same as previously described [11,12]. Planar lipid bilayers were painted onto a 100-μm aperture in a Delrin cup using a 40 mg/ml solution of palmitoyl-oleoyl-phosphatidylserine (POPS) and palmitoyl-oleoyl-phospha-

tidylethanolamine (POPE) (3:1, w/w) in *n*-decane. All of the bathing solutions contained 2 mM $MgCl_2$, 10 mM Hepes (pH 7.4 with CsOH), 1 mM EGTA (pH 7.4 with CsOH), 10 mM MgATP (pH 7.4 with Tris), 30 nM PKA catalytic subunit (Sigma) and Cs^+ salts at the indicated concentration. Vesicles were incubated with 10 mM MgATP and 200 nM PKA catalytic subunit (Sigma) for 10 min on ice before use. Vesicles were painted onto the *cis* side of the planar lipid bilayer using a thin fire-polished glass rod dipped into the membrane vesicle suspension (12 mg protein/ml). Routinely, channel recordings were carried out for 2 min at any set holding potential and were filtered at 60 Hz. Analysis of channel current recordings was performed using the pClamp program (version 5.5, Axon Instruments). Current–voltage relationships were fitted by linear regression. Where stated, *n* indicates the number of channel recordings and *N* indicates the number of bilayers with active CFTR channels from which recordings were made.

2.9. Other materials

The sources of most of the materials were described previously [3,5,11,12]. Yeast strain EGY48 was a gift from Dr. Stephen Crews of the UNC Department of Biochemistry and Biophysics. CFTR baculovirus infected Sf9 cell membrane vesicles were made by Dr. Laura W. Schrum in this laboratory as described previously [5]. Dowex 1X8-100, ATP-γ-S, and all protease inhibitors were purchased from Sigma. Protein determinations were carried out as described previously [3].

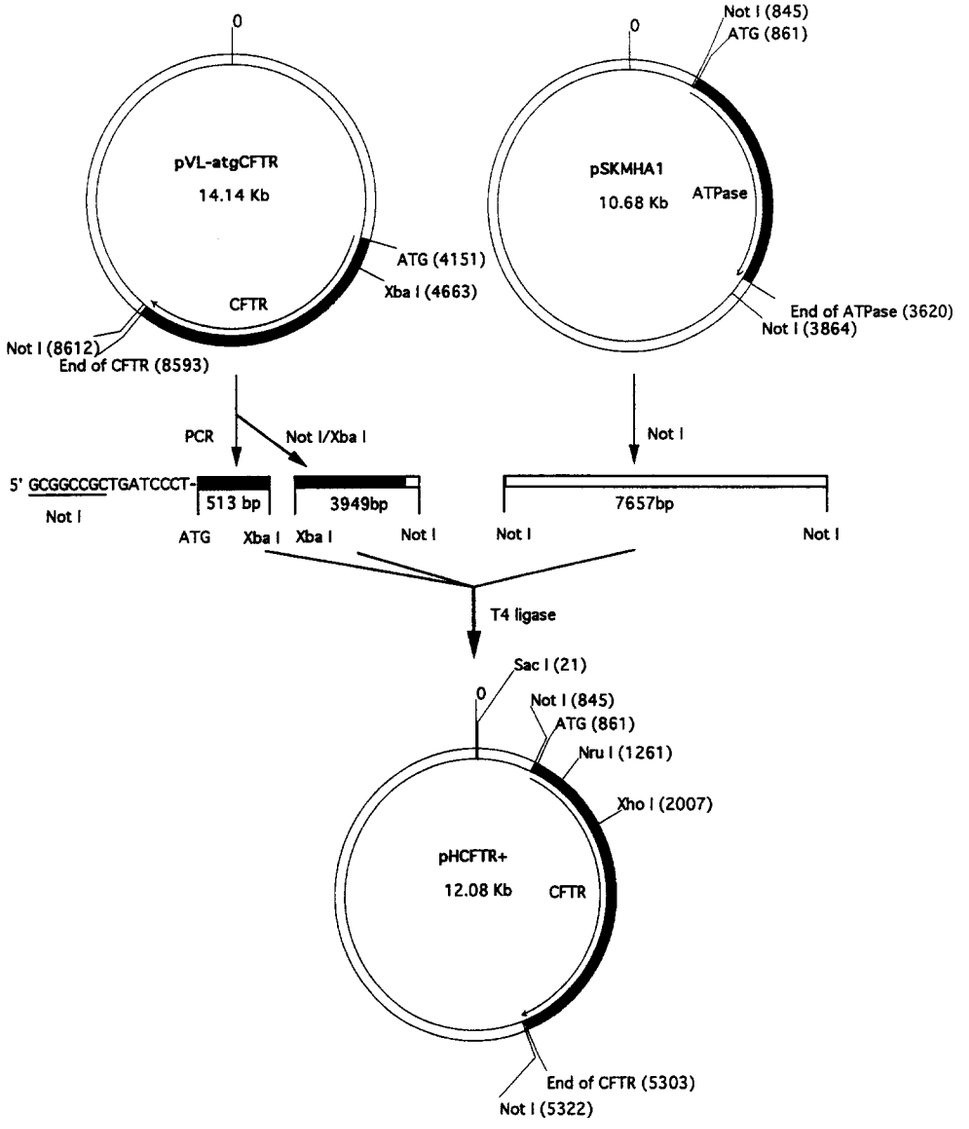

Fig. 1. Construction of pHCFTR + . See text for details. Filled parts represent coding regions of the CFTR or neurospora H^+-ATPase, and the arrows with the filled parts indicate the sense direction of the cDNAs.

3. Results

pHCFTR + , the first plasmid used in these studies, was constructed as outlined in Fig. 1 and described in Section 2. This plasmid was designed on the basis of the neurospora plasma membrane H^+-ATPase expression plasmid pSKMHA1, because this plasmid produces the highest ATPase expression levels among several derivative plasmid constructs made in our previous study [3]. The H^+-ATPase synthesis from pSKMHA1 was proposed to involve initiation at an upstream in-frame ATT rather than the ATG start codon of the neurospora H^+-ATPase. This proposal was based on the observation that the expressed H^+-ATPase of pSKMHA1 is somewhat larger than the native enzyme as judged by SDS-PAGE, and on the fact that the introduction of a frameshift just upstream from the neurospora H^+-ATPase ATG start codon eliminated the molecular weight difference and concomitantly reduced the level of ATPase expression [3]. Since the integrity of the sequence upstream from the ATG start codon of the H^+-ATPase in pSKMHA1 appeared to be critical for high expression levels, an identical sequence was constructed upstream from the ATG start codon of the CFTR in pHCFTR + . Fig. 2 shows some of the key features in this region of pHCFTR + . There are three in-frame ATT's without downstream in-frame stop codons, which are designated ATT1, ATT2, and ATT3, respectively. ATT1 is the most likely ATT at which initiation occurs in plasmid pSKMHA1 [3], because it is the first of the three ATT's, and initiation at this codon would produce an ATPase molecule with a molecular weight closest to that indicated by SDS-PAGE analysis [3].

Fig. 3 (lane 1) shows the level of CFTR expression obtained with strain HCFTR + , produced by transforming the parent strain EGY48 with plasmid pHCFTR + . This transformant produces relatively low levels of the CFTR, and as expected, no CFTR is produced in strain HCFTR − , in which the expression plasmid contains an antisense CFTR coding region (Fig. 3, lane 2). The amount of the CFTR produced in strain HCFTR + is at least as high as

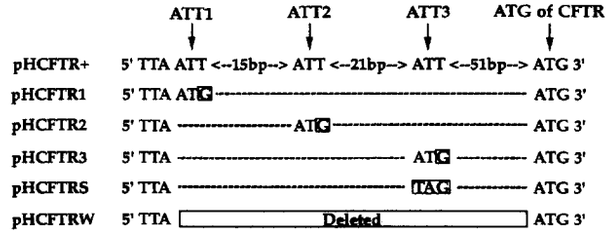

Fig. 2. Sequence differences between pHCFTR + and its derivative plasmids. The sequences differences upstream from the ATG start codon of the CFTR in pHCFTR + and its derivative plasmids are shown. The dashed lines indicate sequences identical to pHCFTR + . Base changes from pHCFTR + are marked with boxes. The upstream fragment of pHCFTR + contains three in-frame ATT's with no following in-frame stop codons is indicated by the arrows. The ATG start codon of the CFTR is also indicated by an arrow.

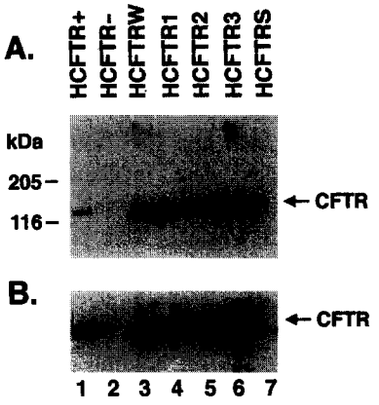

Fig. 3. Expression of the CFTR in various yeast transformants. Twenty μg of total membrane protein from each strain was subjected to 7.5% SDS-PAGE and blotting onto PVDF membrane for immunostaining as described in Section 2. (A) immunostaining pattern detected by enhanced chemiluminescence. (B) the same as (A) but with a prolonged exposure time. The strains used for each lane are indicated at the top. The arrows indicate the 140 kDa CFTR band.

that produced in most animal cell expression systems, and roughly 2% of that produced in the baculovirus Sf9 insect cell system. And, considering the ease with which large quantities of yeast cells can be grown, strain HCFTR + was potentially useful for our planned CFTR purification studies. However, it seemed possible that if CFTR production in strain HCFTR + was initiated at an ATT, production might be increased by changing this codon to an ATG. Thus, the suspected ATT start codon in pHCFTR + , i.e. ATT1, was mutated to an ATG to produce pHCFTR1. And, because it was uncertain as to which, if any, of the ATT's in this region was the actual start codon, each of the other two ATT's were also changed to an ATG to produce pHCFTR2 and pHCFTR3. And finally, because it was not clear whether or not any important regulatory elements are present in this region, the entire region was removed to produce pHCFTRW. As a control for these experiments, a stop codon was introduced in place of ATT3 to produce pHCFTRS. These various changes are summarized in Fig. 2. Fig. 3 shows the levels of the CFTR expressed in the various yeast strains transformed with these plasmids. The relative intensity of immunostaining in Fig. 3A was quantitated by densitometry and computer integration of the peak areas. Taking the greatest value, that from HCFTR3, as 100%, the relative amounts of the CFTR produced in each strain is: HCFTR + , 19%; HCFTRW, 91%; HCFTR1, 63%; and HCFTR2, 75%. Thus, HCFTR1 and HCFTR2 have similar expression levels that are roughly 2–3 times higher than that of strain HCFTR + . And, strains HCFTR3 and HCFTRW produce even greater amounts of the CFTR. Only very small amounts of the CFTR are produced in strain HCFTRS with the stop codon at ATT3.

The strong effect of the ATT to ATG base changes outlined in Fig. 2 on the CFTR expression levels suggested that initiation occurs primarily at the indicated ATG start

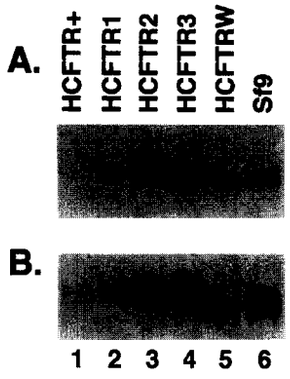

Fig. 4. Relative mobilities of the CFTR expressed in the various strains in an SDS-PAGE gel. Membrane proteins from various strains were subjected to SDS-PAGE and immunoblotting by anti-CFTR antibodies as described in Section 2. In order to obtain higher resolution for proteins with high molecular weight, electrophoresis of the protein samples was carried out in a 5% gel (15×15×0.75-cm) for 6 h at a constant 150 volts. (A) immunostaining by enhanced chemiluminescence. The strains used for each lane are indicated at the top. Lanes 1–4, 20 μg protein; lane 5, 10 μg protein; lane 6, 1 μg protein. (B) the same as (A), but with longer chemiluminescence exposure time to indicate the amounts of the CFTR produced in pHCFTR+.

codons. To further assess this possibility, the CFTRs from the various strains were subjected to high resolution SDS-PAGE to see if they have any detectable mobility differences. The results of such an analysis are shown in Fig. 4. Indeed, small but reproducible mobility differences among the CFTRs of each strain are detectable. The CFTR from strain HCFTRW is the smallest, and those from HCFTR3, HCFTR2, and HCFTR1 are progressively larger. The CFTR from strain HCFTR+ moves close to that from HCFTR2, suggesting that the initiation in HCFTR+ may actually occur at ATT2 instead of ATT1. There is no noticeable mobility difference between the CFTR of strain HCFTRW and that produced in Sf9 insect cells. This suggests that the CFTR produced in yeast is either not glycosylated or is only minimally glycosylated. To confirm this conclusion, a partially purified preparation of the CFTR expressed in yeast was treated with *N*-glycosidase F as described previously [1,5] and the mobility of the CFTR before and after treatment was assessed by SDS-PAGE and immunoblotting (not shown). As a positive control, the glycosylated protein fetuin was added to the incubation mixtures. Whereas the fetuin showed a marked mobility increase as a result of the *N*-glycosidase F treatment, the mobility of the CFTR was unchanged, further indicating that the expressed CFTR contains little, if any, carbohydrate.

Determination of the production level of the CFTR could not be accomplished by direct densitometry of stained SDS-PAGE gels, because the CFTR band in the yeast membranes could not be seen well with Coomassie blue staining, and is difficult to discriminate from other bands in silver-stained gels. Surprisingly, a fairly intense band corresponding to the CFTR is readily visible on Coomassie blue-stained PVDF membrane after electrotransfer for immunodetection. Fig. 5A shows the levels of the CFTR produced in several strains detected on a Coomassie blue-stained PVDF membrane, and Fig. 5B shows the corresponding immunostaining. The shapes of the CFTR bands on the blot (arrows) match exactly with those of the immunostaining, and the Coomassie blue-stained band is seen in membranes from strains HCFTR1, HCFTR2, HCFTR3, HCFTRW and CFTR baculovirus infected Sf9 cells, but not in membranes from strain HCFTRS, which produces extremely small amounts of the CFTR as shown above. The band indicated by the arrow thus represents the CFTR.

Densitometry of the stained blots indicated that the amount of the CFTR in strain HCFTRW is about 1.5% of the total blotted membrane protein. Depending on the relative transblotting efficiency of the CFTR versus the other membrane proteins, this value may over- or underestimate the CFTR yield, although in general, high molecular weight proteins have lower transblotting efficiencies. We therefore quantitated the CFTR yield in a different way. The amount of the CFTR in the Sf9 insect cell membranes is larger than that in the yeast cell membranes and can be estimated by densitometry of silver-stained gels. By this method, the CFTR produced in the Sf9 cells represents about 5% of the total membrane protein. The amount of the CFTR in the membranes of yeast stain HCFTRW is about 5–10% of that in the Sf9 cell membranes as judged by comparison of numerous immunoblots similar to the one shown in Fig. 5. Thus, the CFTR is produced in strain HCFTRW in amounts approx. 0.5% of the total membrane protein. Since strain HCFTRW produces a wild-type CFTR in nearly the highest amounts with no potentially deleterious N-terminal peptide exten-

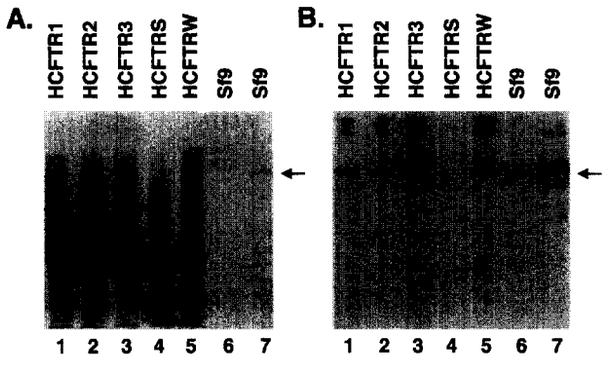

Fig. 5. Quantitation of the amounts of the CFTR produced in several yeast strains and in CFTR baculovirus infected Sf9 insect cells. Membrane protein samples from various cells were run in a 7.5% SDS minigel and transblotted to a PVDF membrane as described in Section 2. The identities of the strains used in each lane are indicated above the lanes. (A) PVDF blot stained with Coomassie blue. (B) corresponding immunostaining by enhanced chemiluminescence. Lanes 1–5 contained 20 μg of yeast membrane protein. Lane 6 and lane 7 contained 0.4 and 2.0 μg of Sf9 cell membrane protein respectively. The arrows indicate the 140 kDa CFTR band.

sion such as that produced in HCFTR3, all subsequent studies were carried out primarily with the CFTR produced in strain HCFTRW.

In order to determine the subcellular distribution of the CFTR expressed in yeast, crude membranes from strain HCFTRW were fractionated by discontinuous sucrose gradient centrifugation. The results of this experiment are shown in Fig. 6. The CFTR is most abundant in light membrane fractions near the top of the gradient, a distribution distinctly different from that of the plasma membrane H^+-ATPase which is enriched near the bottom. Thus, the majority of the expressed CFTR appears not to be directed to the plasma membrane. However, a small amount of the CFTR may comigrate with the plasma membrane.

The next question of interest regards the functionality of the CFTR expressed in yeast. To address this question, we first measured channel activities in isolated membrane vesicles. Chloride channel activities were measured by the $^{125}I^-$ uptake assay described by Ran and Benos [9]. This type of isotope flux assay based on the work of Garty et al. [13] has been used extensively as a rapid functional assay for various channels in native heterologous or reconstituted membrane vesicles, including the CFTR and other chloride channels [9,14–16]. It involves the generation of an inside positive Cl^- diffusion potential which drives the intravesicular accumulation of $^{125}I^-$. Fig. 7 shows the results of a typical vesicle uptake experiment. For these studies, membrane vesicles from strain HCFTRW and HCFTR − were designated as 'CFTR membrane vesicles' and 'control membrane vesicles' respectively. $^{125}I^-$ uptake is observed

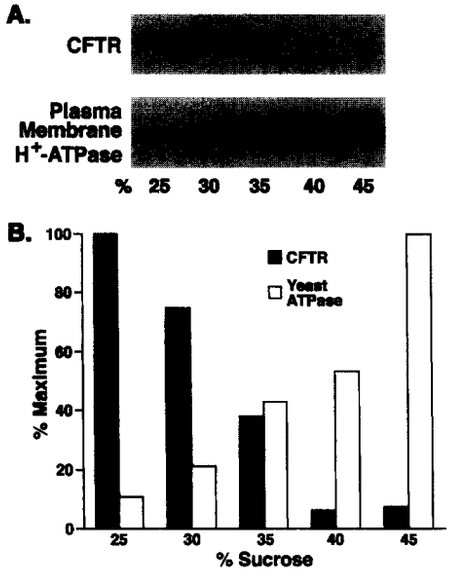

Fig. 6. Subcellular distribution of the CFTR. See Section 2 for details. (A) immunostaining of the CFTR (upper panel) and the yeast plasma membrane H^+-ATPase (lower panel) on the same blot. The numbers under each lane indicates the sucrose concentration of the fraction on top of which the membrane protein was collected. (B) relative immunostaining intensity of each fraction determined by densitometry. The highest value was taken as 100%.

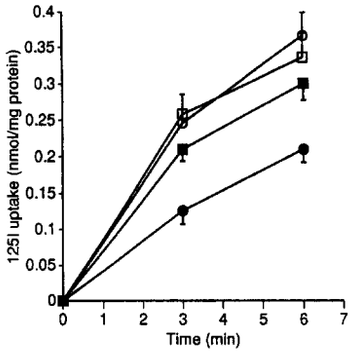

Fig. 7. PKA-activated CFTR channel activity as determined by $^{125}I^-$ uptake into yeast membrane vesicles. The time course of $^{125}I^-$ uptake was determined as described under Section 2. Each point represents an average of 6 measurements on the same membrane vesicle preparation, and each measurement was carried out in duplicate. The error bars are shown in only one direction and indicate the standard error. CFTR membranes alone (●); CFTR membranes plus PKA (◆); control membranes alone (○); control membranes plus PKA (□).

in both the CFTR and control membrane vesicles in the absence of PKA. Collapse of the vesicle membrane potential by the proton conductor, carbonyl cyanide m-chlorophenylhydrazone (CCCP, 50 μM), reduces the $^{125}I^-$ uptake more than 80% in both membrane preparations (not shown), confirming that the $^{125}I^-$ uptake is driven by a transmembrane electrical potential. The addition of PKA increases the $^{125}I^-$ uptake by approx. 30% in CFTR membrane vesicles at 3 min and 6 min. This PKA stimulation is highly significant with P-values at both time points less than 0.01 for 6 experiments on the same membrane preparation, using the unpaired t-test. No PKA stimulation of $^{125}I^-$ uptake is seen in control membrane vesicles ($P > 0.1$). The majority of the $^{125}I^-$ uptake in the absence of PKA in both the CFTR membranes and the control membranes presumably represents endogenous chloride channel activities. These are somewhat variable among membrane preparations and depending on the experiments, may be somewhat greater or somewhat less than shown in Fig. 7. Importantly, if this background activity is subtracted, the PKA stimulation of anion flux in the CFTR membrane vesicles is considerately more dramatic. These results indicate that the expression of the CFTR generates a PKA-activated anion channel in the yeast membrane vesicles.

In order to further confirm the functionality of the CFTR expressed in yeast, and to assess its channel properties, the membrane vesicles were fused to planar lipid bilayers and single channel current recordings were made. Fig. 8A shows typical channel currents recorded using CFTR membrane vesicles in the presence of PKA and ATP under symmetrical conditions with an 800 mM CsCl solution (pH 7.4), on both sides of the bilayer. Channel openings are in the upward direction at positive holding potentials and in the downward direction at negative holding potentials. The current–voltage (I–V) relationship of

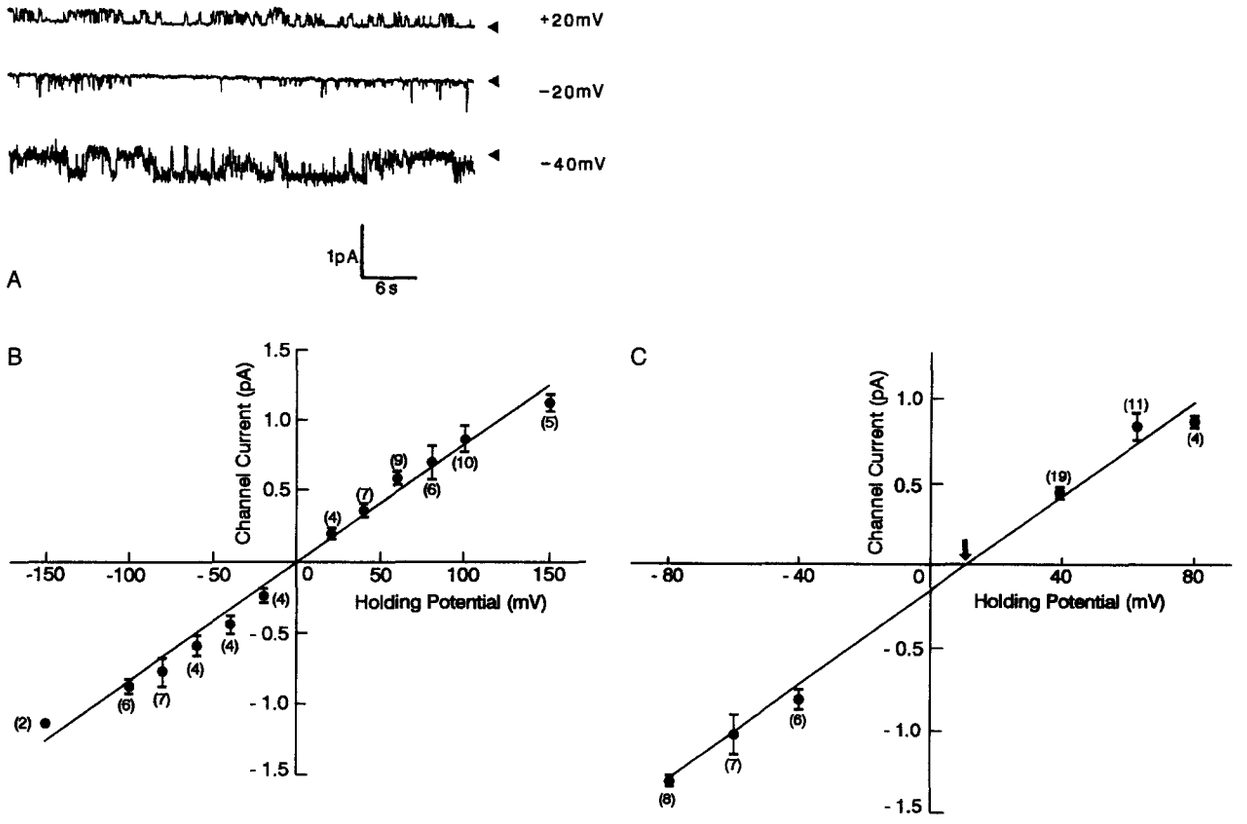

Fig. 8. Electrophysiological characterization of CFTR expressed in yeast using planar lipid bilayer reconstitution. (A) single channel current recordings at different holding potentials under symmetrical 800 mM CsCl conditions. Arrowheads indicate the closed state of the channel. (B) current voltage relationship under symmetrical conditions ($N = 9$). (C) current voltage relationship under asymmetrical (800 mM $CsCl_{cis}$–160 mM $CsCl_{trans}$) conditions ($N = 3$). The arrow indicates the reversal potential (E_R). The data in this figure were all obtained in the presence of PKA and ATP (see Section 2). In (B) and (C) the number of channel recordings (n) is indicated in parentheses beside each point and data is plotted as mean ± standard error.

the channel shown in Fig. 8B is linear (correlation coefficient = 0.99) over the range of −150 mV to +150 mV. Thus, the conductance of the channel shows no voltage-dependence. The slope conductance of the channel is 8.3 ± 0.3 pS ($n = 68$, $N = 9$). To determine whether the channel is cation or anion selective, channel current recordings were made under gradient conditions of 800 mM $CsCl_{cis}$-160 mM $CsCl_{trans}$, and the I–V relationship was then determined (Fig. 8C). Under these conditions with the 5-fold CsCl gradient, there was a rightward shift in the linear I–V relationship with a reversal potential $E_R = 9.3 \pm 0.3$ mV ($n = 54$, $N = 3$), which indicates that the channel is anion-selective. The conductance in this case was 14.2 ± 0.7 pS ($n = 54$, $N = 3$). The discrimination ratio for Cl^-/Cs^+ was determined using the Goldman-Katz-Hodgkin equation [17]. Ionic activities were estimated as

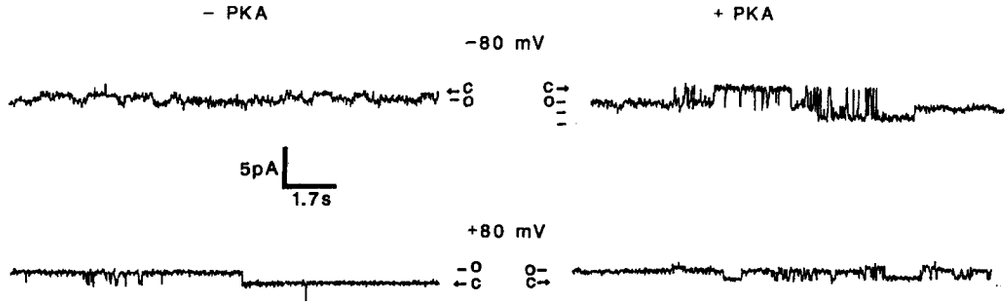

Fig. 9. PKA effect on the CFTR channel activity. On left side of the panel are channel current records obtained at −80 mV and +80 mV holding potential before the addition of PKA. The channel records show one single channel open state with a P_o of 0.20 at −80 mV and 0.29 at +80 mV. On the right side of the panel are channel current records obtained from the same channel 6 min after the addition of PKA catalytic subunit (30 nM) at the same holding potentials. At −80 mV there were 3 channels activated with a Po of 0.33. At +80 mV one channel was active with a P_o of 0.33. MgATP (10 mM) was present in all solutions. c and arrow: closed state of channel; o: open state of channel.

concentration of ion times mean activity coefficient [18]. Based on the measured reversal potential, the channel exhibited a 2:1 discrimination (permeability) ratio for Cl^-/Cs^+. The open probability (P_o) of the channels was determined over the whole range of the holding potentials from −100 mV to +100 mV. The channel P_o showed no voltage dependency and was 0.23 ± 0.02 ($n = 60$, $N = 9$) for this preparation of membranes in the presence of PKA and ATP. (data not shown). As an indication of the relative abundance of the 8 pS channel in the yeast membrane vesicles, the bilayer reconstitution success rate was measured. Out of 42 attempts at bilayer reconstitution with the CFTR membranes, 20 were successful. In two of these a 50-pS channel was observed in addition to the 8-pS channel. In 13 reconstitution attempts with control yeast membranes, no 8-pS channel was seen but one 50-pS channel was observed.

The effect of PKA on channel activity was also investigated. In some vesicle preparations, 8–10 pS channel currents could be observed in the absence of PKA ($N = 4$), presumably as a result of endogenous kinases. These were chosen for experiments to assess the effects of PKA because of the certainty that CFTR channels were present. The results are shown in Fig. 9. Channel currents were first recorded at −80 mV and +80 mV in symmetrical 800 mM CsCl solution with PKA catalytic subunit omitted from both the vesicle suspension and the bilayer chamber solutions. Only single channel currents were observed with P_o of 0.2 ± 0.02 ($N = 3$) and 0.17 ± 0.04 ($N = 4$) at −80 mV and +80 mV holding potentials, respectively. PKA catalytic subunit was then added to the *cis* side of the bilayer. 10 mM MgATP was present in all solutions. Approx. 6 min after PKA addition, the P_o of the channel increased significantly ($P < 0.02$) to 0.32 ± 0.01 ($N = 3$) and 0.31 ± 0.01 ($N = 4$) at −80 mV and +80 mV holding potentials, respectively. In addition, with PKA present, multiple channels of the same size (8–10 pS) were observed (Fig. 9). Therefore PKA not only increased single channel activity, but also increased the number of active channels. These results are similar to those previously reported [19,20]. In five experiments with control membranes, no channel activity was observed before or after PKA addition.

4. Discussion

The results we have obtained demonstrate that functional human CFTR can be expressed in yeast with high yield. Our estimates indicate that the CFTR represents roughly 0.5% of the total yeast membrane protein, a level that approaches that of two ATPases expressed with this system [3,4]. Several factors contributed to this relatively high level of CFTR expression. One important factor was the choice of the yeast strain used for the expression. Strain RS-72 was initially used on the basis of our previous work [3]. In this strain, the constitutive promoter of the yeast plasma membrane H^+-ATPase gene is replaced by a galactose dependent promoter, and thus in glucose media a functional heterologous H^+-ATPase is required for growth because the yeast H^+-ATPase is not synthesized. This selective expression of the endogenous yeast H^+-ATPase is very useful for expression of an exogenous H^+-ATPase but was unnecessary for CFTR expression. It was, in addition, undesirable because the requirement of strain RS-72 for growth in galactose medium precluded the positive regulation of the H^+-ATPase promoter used in this expression system [4]. Thus, in order to obtain glucose-stimulation of the expression and maximize the expression level of the CFTR, strain RS-72 was replaced by strain EGY48, which allows growth on glucose media. This led to a substantial improvement in the level of CFTR expression.

By far the most important factor contributing to high yield expression of the CFTR in the present studies was the optimized arrangement of the bases in the promoter region just preceding the CFTR ATG start codon. Our original construct, pHCFTR+, was based on our most productive neurospora H^+-ATPase expression plasmid, pSKMHA1. In our previous studies with this plasmid, it was concluded that the high level of H^+-ATPase expression is probably due to translation initiation at an in-frame ATT upstream from the neurospora H^+-ATPase ATG start codon [3]. With the likelihood that a more common ATG start codon might be preferred by the yeast translation machinery, each of three candidate upstream ATT's in pHCFTR+ was changed to an ATG. The results were dramatic, with each change leading to a marked increase in the levels of CFTR expression. Importantly, deletion of the most distant ATT and all of the cDNA between it and the CFTR coding sequence was not deleterious, allowing high level expression of native CFTR molecules without an N-terminal extension.

In addition to improving the CFTR expression levels, these results provide additional support for the proposal that translation initiation in this expression system occurs at start codons other than the ATG of the introduced coding sequence [3]. First, the striking effects of a single base change (T to G) on the expression levels from pHCFTR1, pHCFTR2, and pHCFTR3 strongly suggests that each of the mutated ATT's serves as the predominant start codon when replaced by an ATG start codon. The relative sizes of the expressed CFTR's support this interpretation. Second, the introduction of an in-frame TAG stop codon 51 base pairs upstream from the CFTR cDNA in pHCFTR+ abolished nearly all expression, proving that initiation occurs at an upstream initiation site. And third, deletion of the entire fragment from the first of the three potential ATT start codons (ATT1) to the ATG of the CFTR results in one of the highest levels of CFTR expression obtained. In this case, translation initiation must occur at the codon that was originally ATT1. Interestingly,

as mentioned above, the similar mobilities of the CFTR from pHCFTR + and pHCFTR2 suggest that the initiation from pHCFTR + occurs at ATT2, which means that in pHCFTR3, initiation at a downstream ATG (formerly ATT3) somehow overrides initiation at ATT2.

In summary, the mutation studies have revealed several interesting features about the yeast H^+-ATPase promoter-based expression plasmid and the yeast translation machinery. In future studies with this system, attention to in-frame ATT's in the upstream fragments may be important in several ways. First, it can avoid any unexpected and undesired N-terminal extension in the expressed molecule, which may go undetected because of its small size. Second, changes in the upstream bases clearly may be exploited to improve expression levels as we have done in the experiments reported here. And third, N-terminal extensions caused by initiation at the ATT's could be exploited to add flags or tags such as a multi-histidine extension peptide that could facilitate the purification of the expressed protein by metal affinity chromatography.

The unusual staining properties of the CFTR in SDS-PAGE gels observed in these studies are noteworthy. The molecule stains poorly with Coomassie blue in the gels but is quite visible on Coomassie blue-stained PVDF blots. This was observed for the CFTR from both yeast and Sf9 insect cells, and thus seems to be an intrinsic property of the CFTR. One explanation of this curious effect would be an especially high transblotting efficiency of the CFTR, but this does not seem very likely. Alternatively, the CFTR may not be fully denatured under SDS-PAGE gel conditions. The anomalous mobility of the CFTR in SDS-PAGE gels supports this contention. Although its true molecular mass is 168 kDa, it runs as a ca. 140 kDa protein, suggesting that it may not be fully extended. If not, it is possible that some positive amino acid side chains necessary for Coomassie blue binding [21] may be buried in the molecule, possibly lining the anionic ion channel, and thus inaccessible to the dye. Transblotting onto an extremely hydrophobic PVDF membrane may expose these basic amino acid residues and make them more accessible for staining.

The characteristics of the anion selective channel measured in the CFTR membranes are very similar to those previously reported for the CFTR expressed in 3T3 fibroblast cells [20]. These include the conductance (8 pS), open probability (0.23), linear $I-V$ relationship, lack of voltage dependency, regulation by protein kinase A, and the presence of multiple active channels with similar kinetics after PKA addition (Fig. 8A and 9). This channel is not an endogenous channel because it was only observed in membranes containing the CFTR and never in control membranes. These results demonstrate that functional CFTR has been expressed in yeast.

CFTR channel activity has been reported to exhibit a run-down phenomenon in excised patches in patch clamping studies, with channel activities disappearing in 2–5 min. This run-down of the CFTR was attributed to dephosphorylation by phosphatases present in the membranes [22]. Moreover, crude membrane vesicles containing the CFTR from CHO and NIH-3T3 cells [23], and reconstituted membrane vesicles containing purified CFTR from Sf9 insect cells [2] showed no activity in planar bilayers in the presence of ATP alone, and channel activity could only be observed after both PKA and ATP were added. In another report [24], only 1 CFTR channel was recorded in planar lipid bilayers in 20 experiments without the addition of PKA and ATP, whereas 18 channels were detected in 20 experiments after the addition of PKA and ATP. Thus, in general, activated CFTR channels in isolated membrane vesicles are only rarely formed unless PKA and ATP are added. On the contrary, in the study reported here, CFTR channel activity was observed somewhat more frequently in the absence of added protein kinase A. This suggests that the CFTR may already be phosphorylated by endogenous kinases to some extent when the yeast membranes are isolated.

In summary, functional CFTR has been expressed with high yield in a yeast expression system used previously to produce high levels of recombinant transport ATPases. Our modifications of the system increased the expression level many-fold, and these changes may prove to be helpful in the use of this expression system for other membrane proteins. With the high yield and low cost of growing massive amounts of yeast cells, this CFTR expression system may serve as a valuable new source of starting material for the purification of large quantities of the CFTR. Moreover, the well studied and easily manipulated yeast genetics could provide additional experimental tools for studying CFTR structure and function.

Acknowledgements

We would like to thank Dr. Robert A. Nicholas for his helpful suggestions during this work. We are also very grateful to Dr. Stephen Crews and Dr. Andre Goffeau for providing us with the *S. cerevisiae* strain EGY48 and the polyclonal antiserum to the *S. cerevisiae* plasma membrane H^+-ATPase, respectively. This work was supported by NIH Grants DK-45296 (G.A.S.), DK-43816 (J.C.), DK-43377 (J.C.) and CF Foundation R457 (J.C.).

References

[1] Kartner, N., Hanrahan, J.W., Jensen, T.J., Naismith, A.L., Sun, S., Ackerley, C.A., Reyes, E.F., Tsui, L.-C., Rommens, J.M., Bear, C.E. and Riordan, J.R. (1991) Cell 64, 681–691.

[2] Bear, C.E., Li, C., Kartner, N., Bridges, R.J., Jensen, T.J., Ramjeesingh, M. and Riordan, J.R. (1992) Cell 68, 809–818.

[3] Mahanty, S.K., Rao, U.S., Nicholas, R.A. and Scarborough, G.A. (1994) J. Biol. Chem. 266, 17705–17712.

[4] Villalba, J.M., Palmgren, M.G., Berberian, G.E., Ferguson, C. and Serrano, R. (1992) J. Biol. Chem. 267, 12341–12349.

[5] Sarkadi, B., Bauzon, D., Huckle, W.R., Earp, H.S., Berry, A., Suchindran, H., Price, E.M., Olsen, J.C., Boucher, R.C. and Scarborough, G.A. (1992) J. Biol. Chem. 267, 2087–2095.
[6] Sambrook, J., Fritsch, E.F. and Maniatis, T. (1989) Molecular Cloning, 2nd edn., Cold Spring Harbor Laboratory Press, Cold Spring Harbor, New York.
[7] Kunkel, T.A. (1985) Proc. Natl. Acad. Sci. USA 82, 488–492.
[8] Capieaux, E., Rapin, C., Thines, D., Dupont, Y. and Goffeau, A. (1993) J. Biol. Chem. 268, 21895–21900.
[9] Ran, S. and Benos, D.J. (1991) J. Biol. Chem. 266, 4782–4788.
[10] Eckstein, F. (1985) Annu. Rev. Biochem. 54, 367–402.
[11] Sherry, A.M., Cuppoletti, J. and Malinowska, D.H. (1994) Am. J. Physiol. 266 (Cell Physiol. 35), C870–C875.
[12] Cuppoletti, J., Baker, A.M. and Malinowska, D.H. (1993) Am. J. Physiol. 264 (Cell Physiol. 33), C1609–C1618.
[13] Garty, H., Rudy, B. and Karlish, S.J.D. (1983). J. Biol. Chem. 258, 13094–13099.
[14] Dilda, P. and Lelievre, L.G. (1994) J. Biol. Chem. 269, 7801–7806.
[15] Landry, D.W., Akabas, M.H., Redhead, C., Edelman, A., Cragoe, E.J., Jr. and Al-Awqati, Q. (1989) Science 244, 1469–1472.
[16] Middleton, R.E., Pheasant, D.J. and Miller, C. (1994) Biochemistry 33, 13189–13198.
[17] Hille, B. (1992) Ionic Channels of Excitable Membranes Sunderland, M.A., 2nd edn., Sinauer Associates, p. 341.
[18] Robinson, R.A. and Stokes, R.H. (1965) Electrolyte Solutions, Appendix 8.10, Table 15, p. 571, Butterworths, London..
[19] Berger, H.A., Travis, S.M. and Welsh, M.J. (1993) J. Biol. Chem. 268, 2037–2047.
[20] Fisher, H. and Machen, T.E. (1994) J. Gen. Physiol. 104, 541–566.
[21] Groth, S.F. De. ST., Webster, R.G. and Datyner, A. (1963) Biochim. Biophys. Acta 71, 377–391.
[22] Becq, F., Jensen, T.J., Chang, X.-B., Savoia, A., Rommens, J.M., Tsui, L.-C., Buchwald, M., Riordan, J.R. and Hanrahan, J.W. (1994) Proc. Natl, Acad, Sci. USA 91, 9160–9164.
[23] Tilly, B.C., Winter, M.C., Ostedgaard, L. S, O'Riordan, C., Smith, A.E. and Welsh, M.J. (1992) J. Biol. Chem. 267, 9470–9473.
[24] Bradbury, N.A., Cohn, J.A., Venglarik, C.J. and Bridges, R.J. (1994) J. Biol. Chem. 269, 8296–8302.